observed the rapid sequence of initial grain realignments by closely examining successive video frames in DFTEM mode. The frequent observation of the GB-mediated deformation reported here (Figs. 2 and 3) would not have been possible in bright-field TEM conditions because of the inherent difficulty with differentiating the contrast changes caused by GB-related deformations from those caused by the motion of lattice dislocations in small grains (e.g., less than 20 nm).


**References and Notes**

1. J. R. Weertman *et al.*, *Mater. Res. Soc. Bull.* **24**, 44 (1999).
2. C. C. Koch, D. G. Morris, K. Lu, A. Inoue, *Mater. Res. Soc. Bull.* **24**, 54 (1999).
3. H. Van Swygenhoven, *Science* **296**, 66 (2002).
4. J. R. Weertman, in *Nanostructured Materials: Processing, Properties and Applications*, C. C. Koch, Ed. (William Andrews Publishing, Norwich, New York, 2002), pp. 397–421.
5. J. Schiotz, F. D. DiTolla, K. W. Jacobsen, *Nature* **391**, 561 (1998).
6. S. Yip, *Nature* **391**, 532 (1998).
7. J. Schiotz, K. W. Jacobsen, *Science* **301**, 1357 (2003).
8. V. Yamakov, D. Wolf, S. R. Phillpot, A. K. Mukherjee, H. Gleiter, *Nature Mater.* **3**, 43 (2004).
9. C. A. Schuh, T. G. Nieh, T. Yamasaki, *Scripta Mater.* **46**, 735 (2002).
10. M. Ke, S. A. Hackney, W. W. Milligan, E. C. Aifantis, *Nanostructured Mater.* **5**, 689 (1995).
11. C. J. Youngdahl, J. R. Weertman, R. C. Hugo, H. H. Kung, *Scripta Mater.* **44**, 1475 (2001).
12. K. S. Kumar, S. Suresh, M. F. Chisholm, J. A. Horton, P. Wang, *Acta Mater.* **51**, 387 (2003).
13. R. C. Hugo *et al.*, *Acta Mater.* **51**, 1937 (2003).
14. H. V. Swygenhoven, J. R. Weertman, *Scripta Mater.* **49**, 625 (2003).
15. Materials and methods are available as supporting material on *Science* Online.
16. R. Raj, M. F. Ashby, *Metal. Trans.* **2**, 1113 (1971).
17. K. E. Harris, V. V. Singh, A. H. King, *Acta Mater.* **46**, 2623 (1998).
18. D. Moldovan, D. Wolf, S. R. Phillpot, *Acta Mater.* **49**, 3521 (2001).
19. M. Legros, B. R. Elliott, M. N. Rittner, J. R. Weertman, K. J. Hemker, *Philos. Mag. A* **80**, 1017 (2000).
20. V. Yamakov, D. Wolf, M. Salazar, S. R. Phillpot, H. Gleiter, *Acta Mater.* **49**, 2713 (2001).
21. R. Mitra, W.-A. Chiou, J. R. Weertman, *J. Mater. Res.* **19**, 1029 (2004).
22. Z. Budrovic, H. Van Swygenhoven, P. M. Derlet, S. V. Petegem, B. Schmitt, *Science* **304**, 273 (2004).
23. V. Yamakov, D. Wolf, S. R. Phillpot, A. K. Mukherjee, H. Gleiter, *Nature Mater.* **1**, 45 (2002).
24. H. V. Swygenhoven, P. M. Derlet, A. Hasnaoui, *Phys. Rev. B* **66**, 024101 (2002).
25. M. W. Chen *et al.*, *Science* **300**, 1275 (2003).
26. J. P. Hirth, J. Lothe, *Theory of Dislocations* (Wiley, New York, ed. 1, 1982), p. 837.
27. L. E. Murr, *Interfacial Phenomena in Metals and Alloys* (Addison Wesley, Reading, MA, 1975).
28. P. S. Dobson, P. J. Goodhew, R. E. Smallman, *Philos. Mag.* **16**, 9 (1967).


29. Supported by NSF grant CMS-0140317 to the University of Pittsburgh. The work at NCEM/LBNL and at SNL was supported by the Director, Office of Science, Office of Basic Energy Sciences, Division of Materials Sciences and Engineering, of the U.S. Department of Energy. Sandia is a multiprogram laboratory operated by Sandia Corporation, a Lockheed Martin Company, for the United States Department of Energy's National Nuclear Security Agency under contract DE-AC04-94AL85000. We thank L. Lu and C. Y. Song for fruitful discussion.


**Supporting Online Material**

www.sciencemag.org/cgi/content/full/305/5684/654/DC1
Materials and Methods
Fig. S1

5 April 2004; accepted 18 June 2004

# Pinpointing the Source of a Lunar Meteorite: Implications for the Evolution of the Moon


**Edwin Gnos,[1]* Beda A. Hofmann,[2] Ali Al-Kathiri,[1] Silvio Lorenzetti,[3] Otto Eugster,[3] Martin J. Whitehouse,[4] Igor M. Villa,[1] A. J. Timothy Jull,[5] Jost Eikenberg,[6] Bernhard Spettel,[7] Urs Krähenbühl,[8] Ian A. Franchi,[9] Richard C. Greenwood[9]**



**The lunar meteorite Sayh al Uhaymir 169 consists of an impact melt breccia extremely enriched with potassium, rare earth elements, and phosphorus [thorium, 32.7 parts per million (ppm); uranium, 8.6 ppm; potassium oxide, 0.54 weight percent], and adherent regolith. The isotope systematics of the meteorite record four lunar impact events at 3909 ± 13 million years ago (Ma), ~2800 Ma, ~200 Ma, and <0.34 Ma, and collision with Earth sometime after 9.7 ± 1.3 thousand years ago. With these data, we can link the impact-melt breccia to Imbrium and pinpoint the source region of the meteorite to the Lalande impact crater.**


The elevated Th content of the lunar Procellarum terrane was recognized during the Apollo gamma-ray remote mapping program (*1*). The terrane, which includes Mare Imbrium and Mare Procellarum, is characterized by K-REE-P (or KREEP) [potassium (K), rare earth elements (REE), and phosphorus (P)] rock, which is enriched in incompatible elements (*2–5*). Such material was returned by all Apollo missions (*6*). KREEP-rich material is confined to areas surrounding the Imbrium basin and the Montes Carpatus–Lalande belt (*7*), where the impact deposits provide a datable marker of lunar stratigraphy (*6*, *8*). The age of the Imbrium basin has been inferred from isotope-system shock-resetting data and is debated to be either 3770 or 3850 million years old (*9*, *10*).

Sayh al Uhaymir (SaU) 169 is a 206.45-g rock found in the Sultanate of Oman (*11*). The rock consists of two lithologies (Fig. 1). About 87% by volume (estimates based on tomographic sections) (fig. S1) consists of a holocrystalline, fine-grained polymict impact-melt breccia (stage I in Fig. 1) containing 25 to 40 vol % of shocked rock and mineral clasts. The rock clasts are coarse-grained norites, gabbronorites, and mafic granulites. Crystal clasts comprise plagioclase ($An_{57-94}$), orthopyroxene ($En_{44-78}Wo_{1-7}$), olivine ($Fo_{58-67}$), and minor ilmenite, clinopyroxene, spinel, tridymite, or kamacite (table S1). The mineral chemistry of clasts suggests the presence of norites to olivine norites and subordinate, more evolved magmatites (granodiorites to granites) and a few granulites at the impact area. No highland anorthosites ($An_{>97}$) were identified.

The fine-crystalline impact melt (generally <200-μm grain diameter) consists of short-prismatic, low-Ca pyroxene ($En_{61-64}Wo_{3-4}$), mildly shocked plagioclase ($An_{75-81}$), and potassium feldspar, ilmenite, whitlockite, olivine ($Fo_{58-59}$), zircon, troilite, kamacite, and tridymite (see also table S1). The impact melt ilmenites contain unusually high $Nb_2O_5$ (~0.5 wt %), which distinguishes them from known lunar ilmenites (*6*). The impact melt is partially rimmed by shock-lithified regolith (13 vol%). We distinguish two stages of regolith formation (II and III in Fig. 1) from compositional differences. Regolith II and III comprise clasts of crystalline and glassy volcanic rocks, magmatic rocks, breccias, mafic granulites, and crystal fragments. Only stage III regolith is bordered by flow-banded glass and contains yellow and orange glass fragments (including glass beads), olivine basalts, pyroxferroite-bearing basalts, and an anorthosite clast. The basaltic clasts encompass the full range of compositions from Ti-rich to Ti-poor basalts, including aluminous members and picrobasalts (table S2). Glassy shock veins (stage IV in Fig. 1)


[1]Institut für Geologie, Universität Bern, Baltzerstrasse 1, CH-3012 Bern, Switzerland. [2]Naturhistorisches Museum der Burgergemeinde Bern, Bernastrasse 15, CH-3005 Bern, Switzerland. [3]Physikalisches Institut, Abteilung für Weltraumforschung und Planetologie, Universität Bern, Sidlerstrasse 5, CH-3012 Bern, Switzerland. [4]Laboratory for Isotope Geology, Swedish Museum of Natural History, Box 50007, SE-104 05, Stockholm, Sweden. [5]National Science Foundation–Arizona Accelerator Mass Spectrometry Laboratory, University of Arizona, 1118 East Fourth Street, Tucson, AZ 85721, USA. [6]Paul Scherrer Institut, 5232 Villigen, Switzerland. [7]Max-Planck-Institut für Chemie, Abteilung Kosmochemie, 55020 Mainz, Germany. [8]Departement für Chemie und Biochemie, Universität Bern, Freiestrasse 3, CH-3012 Bern, Switzerland. [9]Planetary and Space Sciences Research Institute, Open University, Milton Keynes MK7 6AA, UK.

*To whom correspondence should be addressed: gnos@geo.unibe.ch

crosscut impact melt and regolith and record the latest impact event.

The chemical composition of the meteorite has been characterized by using complementary methods. Nondestructive γ-ray spectroscopy of the uncut rock yielded a typically lunar K/U ratio of 554. The mean of three oxygen isotope measurements of the impact melt ($\delta^{17}O$ = 3.37‰, $\delta^{18}O$ = 6.48‰, and $\Delta^{17}O = 0.001 \pm 0.032$‰) plots on the Earth-Moon fractionation line (*12*). Chemical analyses were obtained from the impact melt, the regolith, and a large breccia clast (Table 1 and Fig. 1). Th, U, and K concentrations are similar for powder aliquots of the impact melt and for the bulk rock. A lunar origin for the meteorite is indicated by lunar element ratios (*6*) such as Fe/Mn (moon, 60 to 80; impact melt, 79; regolith, 78; regolith clast, 74) and K/U ratios (moon, 320 to 3800; impact melt, 535; regolith, 1682; clast, 1253).

The SaU 169 impact-melt breccia is chemically similar to Apollo KREEP impact-melt breccias (*4*), with slightly lower Al and Si, and higher Na, Ti, and P. However, with 32.7 ppm Th, 8.6 ppm U, and 1332 ppm $REE_{tot}$, the impact melt is more enriched in KREEP elements than is any other known lunar rock (*6*). Mean concentrations in Apollo 14 to 17 Th-rich impact-melt breccias range from 8.2 to 16.7 ppm (*13*). Relative to Apollo KREEP-rich impact melts, it is enriched in incompatible trace elements by a factor of 2 to 4 (Fig. 2). The alkali elements K, Rb, and Cs occur at levels typical for Apollo impact melts but are depleted relative to other incompatible trace elements: K/Th, Rb/Th, and Cs/Th are only 0.35 ± 0.02 of the Apollo impact-melt breccia values (Fig. 2), which indicates a decoupling of the alkalis during incompatible trace-element fractionation. A low Rb/Sr of 0.04 shows that it is not related to highly evolved KREEP differentiates (Rb/Sr, 0.10 to 0.56) (*13*). The siderophile elements Ni, Co, Ir, and Au are present at levels similar to Apollo impact melts and require ~0.5% of a meteoritic component.

The average regolith (Fig. 1 and Table 1) has a composition similar to Apollo 12, 14,

**Table 1.** Whole-rock chemistry.

| Oxides or elements | Impact-melt breccia 827 mg* | Average regolith 185 mg† | KREEP clast 117 mg† |
|---|---|---|---|
| | | *wt %* | |
| $SiO_2$ | 45.15 | 46.9‡ | – |
| $Al_2O_3$ | 15.88 | 17.54 | 16.34 |
| $FeO_{tot}$ | 10.67 | 11.09 | 8.80 |
| MnO | 0.14 | 0.14 | 0.12 |
| MgO | 11.09 | 7.94 | 6.92 |
| CaO | 10.16 | 11.72 | 10.60 |
| $Na_2O$ | 0.98 | 0.78 | 1.18 |
| $K_2O$ | 0.54 | 0.46 | 0.88 |
| $TiO_2$ | 2.21 | 2.49 | 1.47 |
| $ZrO_2$ | 0.38 | 0.08 | 0.19 |
| BaO | 0.17 | 0.07 | 0.15 |
| $Cr_2O_3$ | 0.14 | 0.19 | 0.12 |
| $P_2O_5$ | 1.14 | 0.42 | 0.76 |
| S | 0.33 | | |
| Total | 98.98 | 99.82 | |
| | | *ppm* | |
| Sc | 25 | 28 | 18 |
| V | 36 | 61 | 36 |
| Cr | 992 | 1310 | 811 |
| Co | 31 | 19 | 12 |
| Ni | 204 | 82 | 58 |
| Cu | 9 | <20 | <20 |
| Zn | 31 | <60 | <60 |
| Rb | 13.7 | 10.0 | 20.0 |
| Sr | 359 | 214 | 230 |
| Y | 532 | 162.5 | 338 |
| Zr | 2835 | 596 | 1397 |
| Nb | 124 | 18 | 112 |
| Cs | 0.8 | 0.4 | 0.9 |
| Ba | 1520 | 593 | 1351 |
| La | 170 | 52 | 113 |
| Ce | 427 | 139 | 297 |
| Pr | 57.45 | 17.1 | 35.6 |
| Nd | 256.5 | 76.9 | 162 |
| Sm | 70.15 | 21.9 | 44.9 |
| Eu | 4.20 | 2.43 | 2.45 |
| Gd | 86.4 | 25.3 | 50.4 |
| Tb | 15.1 | 5.08 | 10.5 |
| Dy | 94.15 | 30.7 | 63.9 |
| Ho | 21.3 | 6.36 | 13 |
| Er | 58.05 | 18.6 | 39.3 |
| Tm | 9.13 | 2.72 | 5.96 |
| Yb | 54.65 | 16.9 | 36 |
| Lu | 7.64 | 2.53 | 5.24 |
| Hf | 64.3 | 14.8 | 34.7 |
| Ta | 7.1 | 2.14 | 4.16 |
| W | 3.45 | 1.3 | 2.5 |
| Ir ppb | 4.2 | | |
| Au ppb | 6 | | |
| Pb | 13.8 | <10 | <10 |
| Th | 32.7 | 8.44 | 21.70 |
| U | 8.6 | 2.27 | 5.83 |
| Sum REE (ppm) | 1332 | 418 | 879 |
| Fe/Mn (wt) | 76.5 | 79.5 | 73.6 |
| Mg/(Fe+Mg) (mol) | 0.65 | 0.56 | 0.58 |
| K/U (wt) | 521 | 1682 | 1253 |
| Th/U (wt) | 3.80 | 3.72 | 3.72 |

*Combined inductively coupled plasma mass spectrometry and optical emission spectrometry, and instrumental neutron activation analysis. †Inductively coupled plasma mass spectrometry and optical emission spectrometry. ‡Microprobe value on regolith shock glass.

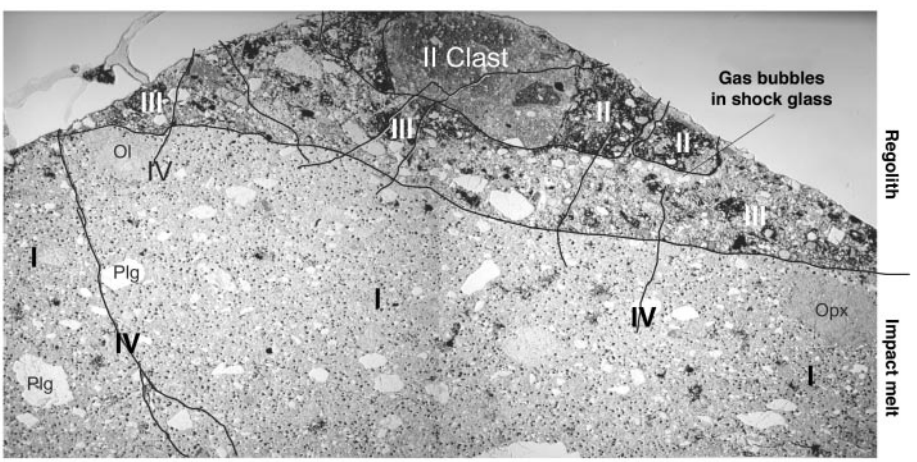


**Fig. 1.** Thin-section photograph showing the different lithologies and their age relationship: I, impact-melt breccia. II and III, two types of regolith (III intrudes II). IV designates shock veins as youngest formation. Ol, olivine; Plg, plagioclase; Opx, orthopyroxene. Image width is 35 mm.

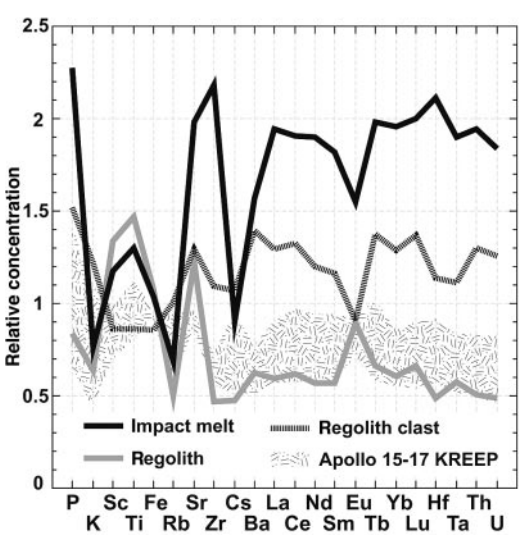


**Fig. 2.** Element abundances of impact-melt breccia, regolith II and III combined, and a polymict breccia clast in regolith II normalized to average Apollo 14 high-Th impact-melt breccias (*13*). Data for Apollo 15 to 17 impact melts are shown for comparison. Compared with Apollo data, P, Zr, REE, Th, and U contents are significantly higher, but K, Cs, and Rb, as well as Al and Si (typically fractionated in potassium feldspar), are lower.

and 15 regoliths. In contrast to the impact melt, the regolith is not depleted in Na and K (Fig. 2), as shown by the higher K/U of 1682. The regolith clast is an evolved KREEP rock (Fig. 2) with 21.7 ppm Th, but it is unrelated to the impact melt, on the basis of its K/U ratio of 1253. The exceptionally high Th, U, and K contents restrict the provenance of SaU 169 to the Imbrium area (*13*).

We determined the ages of the four impact events using isotopic data. $^{207}$Pb-$^{206}$Pb isotope ratios (table S3) were obtained in thin section by ion-microprobe analysis on 12 poikilitic impact-melt zircons and yielded a crystallization age of 3909 ± 13 Ma [2σ; mean square weighted deviation (MSWD), 0.33] (Fig. 3). $^{39}$Ar-$^{40}$Ar data (table S4) were obtained on a feldspar concentrate from the impact melt. The irregular age spectrum in combination with the Ca/K concentrations indicate a resetting of the Ca-rich feldspars at ~2800 Ma and a younger disturbance at <500 Ma affecting the potassium feldspars (fig. S2).

The duration of cosmic-ray exposure (CRE) of the impact-melt breccia and the younger regolith (stage III in Fig. 1) was obtained from light noble gas isotopic characteristics (table S5). All three samples analyzed show He loss; hence, the $^{3}$He CRE age is not significant. The production rates for $^{21}$Ne and $^{38}$Ar depend on the chemical composition and on shielding depth during exposure to cosmic rays. The $(^{22}Ne/^{21}Ne)_c$ value of 1.197 for the impact melt and 1.200 for the regolith indicate irradiation at a shielding depth of a few tens of centimeters. Using the method for calculating production rates proposed by (*14*) at the lunar surface and (*15*) during transfer in space, and assuming a typical shielding of 40 g/cm$^2$, we obtained lunar surface CRE ages from $^{21}$Ne and $^{38}$Ar of 200 ± 40 Ma and 182 ± 36 Ma for the impact melt, and 150 ± 30 Ma and 192 ± 38 Ma for the regolith. The $^{38}$Ar CRE age extracted from the $^{39}$Ar-$^{40}$Ar data is also 192 ± 20 Ma (table S4 and fig. S2).

By adopting a saturation activity for $^{10}$Be of 25 dpm/kg as given by (*16*), we found the upper time limit for a small rock exposure during Moon-Earth transfer, estimated from $^{10}$Be (table S6), to be 0.34 Ma. Thus, the exposure in free space is negligibly short compared with the total CRE. We conclude that the CRE ages are lunar regolith residence times. Like most lunar meteorites (*17*), SaU 169 thus seems to have resided in the upper meter of the regolith before launch into space, as supported by our CRE ages and by the solar wind component found in the stage III regolith (table S5). The terrestrial age obtained by $^{14}$C and $^{10}$Be methods is ≤9700 ± 1300 years (table S6).

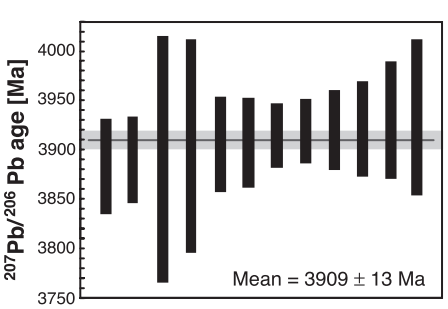


**Fig. 3.** $^{207}$Pb/$^{206}$Pb ages of 12 zircons from the impact melt. Data are corrected for common Pb (*24*) and yield a weighted average age of 3909 ± 13 Ma (2σ; MSWD = 0.33).

The combined age data indicate a complex lunar history. Crystallization of the impact melt occurred at 3909 ± 13 Ma, followed by exhumation by a second impact at ~2800 Ma, which raised the sample to a regolith position at unconstrained depth. A third impact at ~200 Ma moved the material closer to the lunar surface, where it mixed with solar-wind–containing regolith. It was launched into space by a fourth impact at <0.34 Ma.

The 3909 ± 13 Ma $^{207}$Pb-$^{206}$Pb zircon age on the impact melt is an accurate estimate for the Imbrium impact event. The small difference from the 3770 ± 20 or 3850 ± 20 Ma range obtained by whole-rock $^{39}$Ar-$^{40}$Ar system (*9*, *10*, *18*) confirms that the argon system yields reliable age estimates. The age difference may reflect the imprecisely known $^{40}$K decay constant. A recalculation of the argon ages with the decay value proposed by (*19*) results in a ~1% age increase.

We were able to constrain the SaU 169 provenance even more tightly by using Lunar Orbiter images in combination with Clementine-derived Fe-Ti maps, Lunar Prospector Th maps, Clementine color-ratio images (750/950 nm), lunar crater ages (*20*, *21*) (table S7), and data from the Apollo and Luna missions. The source location is based on the following assumptions: (i) The high Th (32.7 ppm) impact melt is derived from one of the highest Th areas defined by Lunar Prospector γ-ray mapping; (ii) The regolith Fe-Ti-Th concentrations are representative of the regolith of the ejection area; (iii) The age disturbances at ~2800 and 200 Ma were caused by impacts that were able to disturb the Ar system; (iv) The ejection crater from which the rock was launched to Earth is on the order of a few kilometers (*17*).

The Lunar Prospector γ-ray mapping demonstrated that the surface occurrence of KREEP is confined to the near-side Procellarum terrane (*2*–*5*, *22*, *23*). Because the bulk Th content of the impact melt (Table 1) is higher than any pixel of the Lunar Prospector measurements (maximum, 9.36 to 10.40 ppm) (*7*), we assume that SaU 169 must come from one of the Th hot spots (fig. S3), which are located at the Aristarchus and Aristillus craters, the Montes Carpathus–Fra Mauro region, and the Lalande crater region (*7*). Among these Th hot spots, only the area around Lalande and southeast of the crater Aristillus are compatible with our regolith Fe-Ti-Th concentrations (table S7). In both areas, a young (bright-halo), small crater as a possible launch-to-Earth crater is evident. However, the age data for SaU 169 render the Lalande crater area (9°W 5°S) the most plausible because it contains a ~2800 Ma crater (Lalande, 2246 to 2803 Ma) and a ~200 Ma crater (e.g., Lalande A, 175 to 300 Ma) (table S7). Based on the comprehensive data set presented, we conclude that an origin from the Lalande crater area is most likely.

SaU 169 is the only large high-KREEP sample for which simultaneous determinations of precise age and chemistry are available. The Imbrium impact age dates a strong decline of large impacts in the inner solar system corresponding to the beginning of life-supporting conditions on Earth.

### References and Notes

1. A. E. Metzger, J. I. Trombka, L. E. Peterson, R. C. Reedy, J. R. Arnold, *Science* **179**, 800 (1973).
2. L. A. Haskin, J. L. Gillis, R. L. Korotev, B. L. Jolliff, *J. Geophys. Res.* **105**, 20403 (2000).
3. B. L. Jolliff, J. J. Gillis, L. A. Haskin, R. L. Korotev, M. A. Wieczorek, *J. Geophys. Res.* **105**, 4197 (2000).
4. R. L. Korotev, *J. Geophys. Res.* **105**, 4317 (2000).
5. M. A. Wieczorek, R. J. Phillips, *J. Geophys. Res.* **105**, 20417 (2000).
6. G. H. Heiken, D. T. Vaniman, B. M. French, *Lunar Source Book: A User's Guide to the Moon* (Cambridge University Press, Cambridge, 1991).
7. D. J. Lawrence *et al.*, *Geophys. Res. Lett.* **26**, 2681 (1999).
8. D. E. Wilhelms, *U.S. Geol. Survey Prof. Pap.* **1348**, 1 (1987).
9. B. A. Cohen, T. D. Swindle, D. A. Kring, *Science* **290**, 1754 (2000).
10. D. Stöffler, G. Ryder, *Space Sci. Rev.* **96**, 9 (2001).
11. S. Russell *et al.*, *Meteorit. Planet. Sci.* **38**, A189 (2003).
12. U. Wiechert *et al.*, *Science* **294**, 345 (2001).
13. B. L. Jolliff, *Int. Geol. Rev.* **40**, 916 (1998).
14. C. Hohenberg, K. Marti, F. Podosek, R. Reedy, J. Shirck, *Proc. Lun. Planet. Sci. Conf. 9th*, 2311 (1978).
15. O. Eugster, T. Michel, *Geochim. Cosmochim. Acta* **59**, 177 (1995).
16. C. Tuniz *et al.*, *Geophys. Res. Lett.* **10**, 804 (1983).
17. P. H. Warren, *Icarus* **111**, 338 (1994).
18. G. B. Dalrymple, G. Ryder, *J. Geophys. Res.* **101**, 26069 (1996).
19. K. Min, R. Mundil, P. R. Renne, K. R. Ludwig, *Geochim. Cosmochim. Acta* **64**, 73 (2000).
20. R. B. Baldwin, *Icarus* **71**, 19 (1987).
21. R. B. Baldwin, *Icarus* **61**, 63 (1985).
22. R. C. Elphic *et al.*, *J. Geophys. Res.* **107**, **E4**, 8-1 (2002).
23. W. C. Feldman, O. Gasnault, S. Maurice, D. J. Lawrence, R. C. Elphic, *J. Geophys. Res.* **107, E3**, 5-1 (2002).
24. Materials and methods are available as supporting material on *Science* Online.
25. Funded by Swiss National Foundation grants 21-64929.01, 20-61933.00, and credit 21-26579.89. Thanks to H. Al-Azri and K. Musallam for support; to L. R. Gaddis, USGS, for Lunar Orbiter images; and to J. Kramers, J. Ridley, L. Diamond, D. Fleitmann, T. Armbruster, and B. Hacker for reviews.

**Supporting Online Material**

www.sciencemag.org/cgi/content/full/305/5684/657/DC1
Materials and Methods
SOM Text
Figs. S1 to S3
Tables S1 to S7
References

21 April 2004; accepted 4 June 2004